Available online at www.sciencedirect.com
ScienceDirect
Tetrahedron: Asymmetry
Tetrahedron: *Asymmetry* 18 (2007) 925–930

Absolute configuration of hypothemycin and 5′-*O*-methylhypothemycin from *Phoma* sp.—a test case for solid state CD/TDDFT approach☆

Hidayat Hussain,[a] Karsten Krohn,[a,*] Ulrich Flörke,[a] Barbara Schulz,[b] Siegfried Draeger,[b] Gennaro Pescitelli,[c] Piero Salvadori,[c] Sándor Antus[d,e] and Tibor Kurtán[d]

[a]*Department of Chemistry, Universität Paderborn, Warburgerstraße 100, 33098 Paderborn, Germany*
[b]*Institut für Mikrobiologie, Technische Universität Braunschweig, Spielmannstraße 7, 31806 Braunschweig, Germany*
[c]*Università di Pisa, Dipartimento di Chimica e Chimica Industriale, via Risorgimento 35, 56126 Pisa, Italy*
[d]*Department of Organic Chemistry, University of Debrecen, PO Box 20, H-4010 Debrecen, Hungary*
[e]*Research Group for Carbohydrates of the Hungarian Academy of Sciences, PO Box 55, H-4010 Debrecen, Hungary*

Received 31 January 2007; accepted 12 April 2007

Abstract—Two metabolites, the known antitumor macrolide hypothemycin **1** and its new 5′-*O*-methyl ether, 5′-*O*-methylhypothemycin **2**, and the known steroid ergosterol **3**, were isolated from a *Phoma* sp. The structures were elucidated by means of spectroscopic data analysis, and the absolute configuration of hypothemycin **1** was confirmed by single crystal X-ray analysis in combination with the new solid-state CD/TDDFT methodology. Since the solid-state CD spectrum shows contributions from intermolecular interactions in the crystal, **1** represents a critical test case for our solid-state CD/TDDFT approach.

1. Introduction

Hypothemycin is a 14-membered β-resorcylic acid macrolactone which has been isolated from the fungal fermentations of *Hypomyces trichothecoides*,[2,3] *Hypomyces subiculosis*,[4] *Coriolus versicolor*,[5] and *Aigialus parvus*.[6] The macrolide exhibited moderate antimalarial and antifungal activity, as well as cytotoxicity against various murine and human cell lines.[5,7] It has also been demonstrated to suppress the growth of murine and human tumor cells transplanted into the backs of mice.[8] Both in vitro and in vivo studies by Zhao et al.[9] and Schirmer et al.[7] have identified hypothemycin as a potent and selective inhibitor of the threonine/tyrosine-specific kinase, MEK, and other protein kinases that contain a conserved cysteine residue in their ATP binding site. Since many of these kinases play an important role in signal transduction pathways that regulate cell proliferation, cell differentiation, and apoptosis,[10–12] their aberrant activation can lead to uncontrolled cell proliferation and transformation.[13] Hence, compounds that are specific inhibitors of these target proteins are promising candidates as anticancer agents. Due to the biological importance of the molecule, two independent syntheses have recently been published.[14,15] In a series of preliminary screenings, the culture extract of *Phoma* sp. displayed excellent fungicidal activity, particularly against *Phytophthora infestans*, as well as moderate algicidal, antibacterial, antialgal, and herbicidal activities. To obtain preliminary structural information on the active constituents, the ethyl acetate extract of the fungal cultivation was subjected to column chromatography. We isolated three metabolites, the known macrolide, hypothemycin **1**, a new hypothemycin analogue, 5′-*O*-methylhypothemycin **2**, and the known steroid ergosterol **3**. The absolute configuration of hypothemycin **1** had been tentatively determined by X-ray analysis using anomalous dispersion of oxygen atoms,[5] and then by X-ray analysis of an aigialomycin C4-bromobenzoyl derivative, chemically correlated to hypothemycin.[6] Later, the absolute configuration was also confirmed by stereospecific total synthesis of **1**.[14,15] Having

☆ Biologically Active Secondary Metabolites from Fungi, Part 30. Part 29 lit.[1]

* Corresponding author. Tel.: +49 5251 602172; fax: +49 5251 603245; e-mail: k.krohn@uni-paderborn.de

0957-4166/$ - see front matter © 2007 Elsevier Ltd. All rights reserved.
doi:10.1016/j.tetasy.2007.04.005

independently determined the relative configuration of **1** by X-ray analysis, we applied our solid state CD/TDDFT methodology[1,16–18] to test the new procedure on a molecule endowed, from our perspective, with two interesting properties. First, the 14-membered ring may be expected to be rather conformationally flexible. In such a case, the conventional approach referring to the solution state requires the entire set of CD spectra from all conformations to be computed by TDDFT[19,20] or other quantum mechanical methods,[21,22] weighted by the Boltzmann procedure, and then compared with the solution CD spectrum.[23] In contrast, in our solid-state CD/TDDFT approach, the Cartesian coordinates of the X-ray data serve as input geometry for TDDFT calculation of the theoretical CD spectrum, which is then compared with the CD spectrum recorded in the solid state. In this way, the whole conformational search step is skipped and any geometrical uncertainty avoided. Moreover, theoretical and experimental spectra are expected to give a good match,[1,16–18] since the calculated and the experimentally acquired data are derived from the very same single conformation of the solid state. This approach was first introduced by some of us employing semi-empirical calculations of CD spectra,[16] and later improved by switching to TDDFT calculations which greatly broadened the scope of this method.[1,17,18]

The main prerequisite for the application of the present approach is that the solid-state CD be essentially of a molecular origin, since the calculation is run on a single molecule. Therefore, CD effects intrinsic to the solid state must be negligible, which may arise, for example, from intermolecular couplings between molecules tightly packed in the crystal.[24,25] The analysis of hypothemycin **1** thus offers the possibility to test the validity of the method in the presence of strong chromophores such as β-resorcylate, which in principle may give efficient couplings of the exciton and/or of the magnetic–electric types,[26] potentially limiting our CD/TDDFT approach.

2. Results and discussion

The endophytic fungus *Phoma* sp. (internal strain no. 7133) was isolated from *Senecio kleinii* from Gomera (Spain) and cultivated at room temperature on biomalt solid agar medium for 28 days. The 4 L culture medium was then extracted with ethyl acetate to afford 4.3 g of a crude extract. The crude extract of *Phoma* sp. showed excellent fungicidal activity, particularly against *Phytophthora*, as well as moderate algicidal, antibacterial, antialgal, and herbicidal activities. Column chromatography on silica gel of the fungal ethyl acetate extract led to the isolation of three metabolites, **1**–**3**.

Hypothemycin **1** (Fig. 1), molecular formula $C_{19}H_{22}O_8$, showed maxima in the UV spectrum near 220, 265, and 307 nm, typical of the 4-methoxy, resorcylic acid lactone macrolide chromophore present in the radicicol derivatives.[3] The IR spectrum showed the presence of a highly chelated lactone carbonyl peak at 1620 cm^{-1}. Comparison of the ^1H and ^{13}C NMR spectroscopic data of **1** with those of hypothemycin, a macrolide previously isolated from *Coriolus versicolor*,[5] proved the identity of the compounds. The structure of hypothemycin **1** was further confirmed by X-ray diffraction analysis of a single crystal obtained from EtOAc and *n*-hexane (Fig. 2). As the atomic coordinates derived by Agatsuma et al.[5] are not available from the CCDC database, we have deposited our data therein.[27]

The solution and solid-state CD spectra of hypothemycin **1** were very similar (Fig. 3), although some differences emerged. In the solid-state CD spectra recorded as KCl or KBr disc, a new negative CD transition appeared at 226 nm, and three transitions were observed above 285 nm instead of the 305 nm trough and 333 nm peak of the solution CD spectrum. The individual solid-state CD spectra were obtained as the average of four slightly different CD spectra recorded with 90° rotation of the KCl or

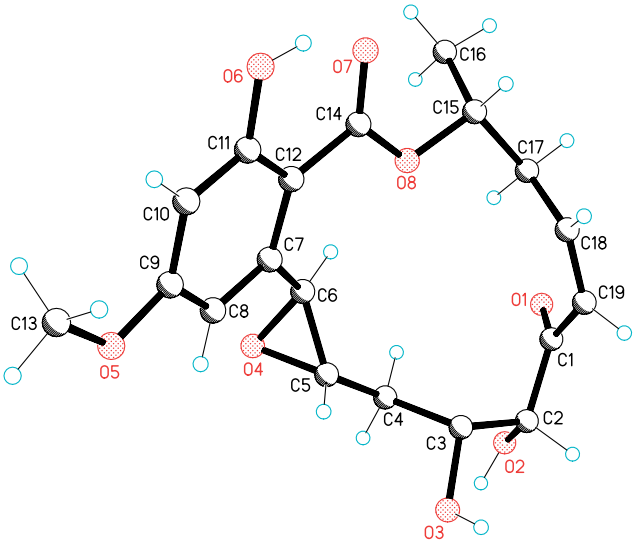

Figure 2. Molecular structure of hypothemycin **1** in the crystal.

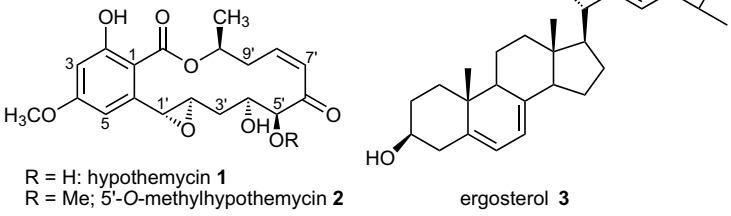

R = H: hypothemycin **1**
R = Me; 5'-*O*-methylhypothemycin **2**

ergosterol **3**

Figure 1. Structures of compounds isolated from *Phoma* sp.

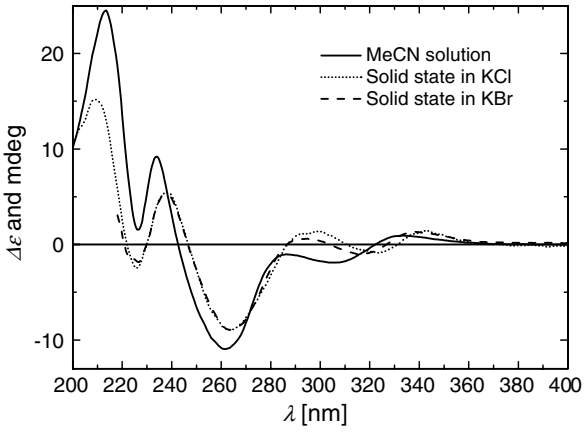

Figure 3. Measured CD spectra of hypothemycin **1** in acetonitrile (solid line), as KCl disc (dotted line) and as KBr disc (dashed line).

KBr disc. The KCl solid-state CD spectrum could be well reproduced with a new disc; a change in the ratio of the sample and KCl affected only the intensities of the transitions, but not the wavelength positions of the maxima. Moreover, the solid-state CD spectra recorded as KCl and KBr disc were practically the same. These results allowed us to exclude the artifacts of the disc as a reason for the observed differences between the solution and solid-state CD spectra. Their origin must therefore be sought in either conformational differences or in effects intrinsic to the crystalline state; the following computational investigation demonstrates that these two sources are both feasible and probably concurrent.

A thorough conformational search was carried out on **1** with molecular mechanics MMFF and semi-empirical AM1 methods. Surprisingly, a very restricted number of low-energy minima was found. In particular, with AM1, a distinctive absolute minimum was isolated (**1A** in Figure 4, plus the rotamer with 4-methoxy flipped by 180°); the second minimum had +1.7 kcal/mol energy (**1B**, plus the 4-methoxy rotamer), while other minima had energies above 2.5 kcal/mol and were not considered. Apparently, the presence of many unsaturations and especially of the *cis*-double bond within the large macrocycle provides an unexpected rigidity. However, a clear-cut conformational picture in solution could not be gained at the present level of investigation. First, simple NMR data such as vicinal ^{1}H–^{1}H *J*-coupling constants were insufficient to discriminate between the quite different structures **1A** and **1B**, for which the measurement of heteronuclear couplings probably would be necessary. Second, the AM1 absolute minimum **1A** is also slightly different from the crystal structure **1ss** (Fig. 4): the root-mean-square deviation for heavy atoms is 0.74 Å. Thus, although the situation emerging from conformational searches is less complicated than expected, employing the solid-state geometry for the CD calculation was still useful for resolving the residual structural ambiguity.

Figure 5a shows CD spectra calculated on the solid-state geometry, (1′*R*,2′*R*,4′*S*,5′*S*,10′*S*)-absolute configuration, with the B3LYP/TZVP method and different values for the Gaussian band-width σ, used to generate full CD spectra from the computed rotational strengths. A second DFT functional, PBE0, gave consistent results.[28] Comparison with the solid-state experimental spectrum (Fig. 5b) reveals good agreement over a large part of the measured wavelength range; thus, the absolute configuration of hypothemycin **1** is independently confirmed as above. Even in the presence of the β-resorcylate chromophore, the application of our solid-state TDDFT/CD approach remains practical (another example involving strong chromophores may be found in the literature[17]).

Clear discrepancies are observed between computed and solid-state experimental spectra only in the two regions (I and II in Fig. 5b) around 285 nm (negative instead of positive band, independent of σ) and 220 nm (trough instead of negative minimum, if $\sigma > 2700\ cm^{-1}$). In our opinion, these discrepancies should not be ascribed to computational inaccuracy. In fact, the first 17 transitions responsible for the CD spectrum above 200 nm all involve virtual orbitals with negative eigenvalues and have energies within 5.92 eV, below the estimated ionization potential of 6.23 eV. These two criteria[29] usually ensure an accurate

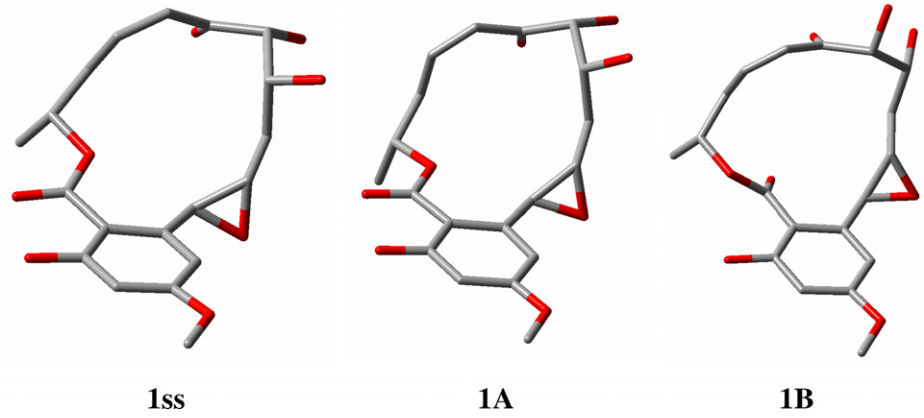

Figure 4. Comparison between the solid-state geometry of hypothemycin **1ss** and AM1-computed minima (**1A**: absolute minimum; **1B**: +1.7 kcal/mol). Hydrogens removed for clarity.

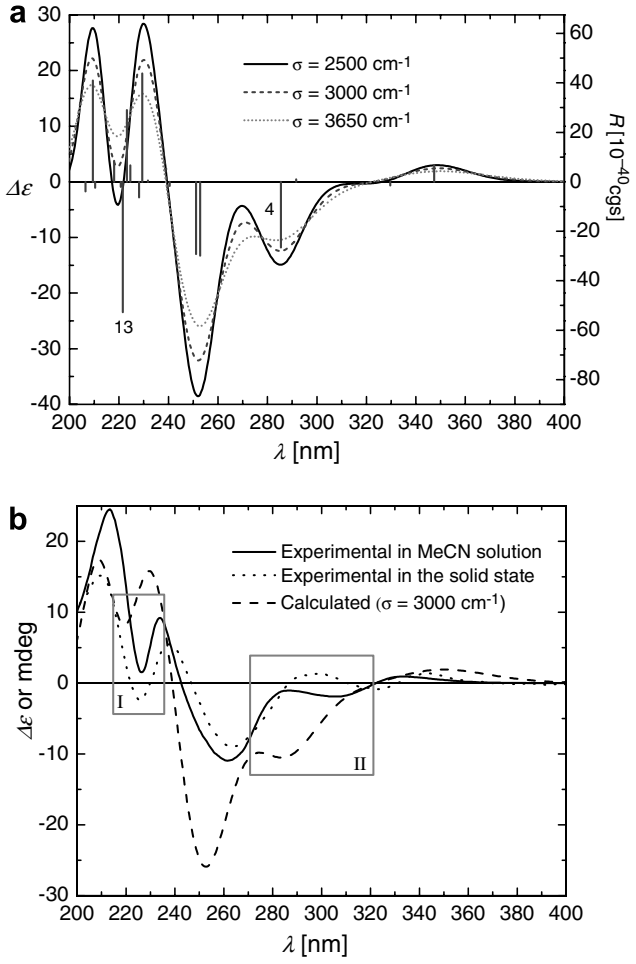

Figure 5. (a) TDDFT-calculated CD spectra for (1′*R*,2′*R*,4′*S*,5′*S*,10′*S*)-hypothemycin **1**, using the solid-state geometry and B3LYP/TZVP method; vertical bars represent rotational strengths *R*. The three curves were generated with different values of the Gaussian band-width σ. (b) Comparison between experimental and calculated spectra.

estimation of electronic excitations and rotational strengths with TDDFT.[1,16–18] Instead, we noticed that in the regions of discrepancy I and II (Fig. 5b), the computed spectra more closely resemble the experimental solution CD than the solid-state one, despite the fact that the solid-state structure was used as input in the calculations. We realized that transitions no. 4 and no. 13, which fall in these regions, are both of aromatic π–π^* character. In general, π–π^* transitions of aromatic chromophores, endowed with large dipole strengths (computed oscillator strengths *f* for no. 4 and no. 13 are 0.15 and 0.10, respectively), may give rise to non-negligible intermolecular interactions if two or more molecules are brought sufficiently close to each other. The crystal unit cell of **1** comprises four distinct molecules, two of which are arranged with aromatic rings lying very close to each other (center-to-center distance 6.9 Å; shortest distance 3.9 Å, between two oxygen atoms O5···O6). We therefore infer that the differences between calculated and experimental solid-state CD spectra around 220 and 285 nm are due to intermolecular couplings; similarly, we ascribe the differences seen between the experimental spectra (Fig. 3) in the corresponding regions mainly to the same source, although conformational differences may also play some role.

In conclusion, we consider compound **1** as a borderline case for our solid-state CD/TDDFT approach: assignment of the absolute configuration is still unambiguously feasible; however, the presence of chromophoric systems such as that in **1**, or stronger, must alert us to spectral features possibly deviating from the computations.

Compound **2** has the molecular formula $C_{20}H_{24}O_8$ as deduced from HREIMS and ^{13}C NMR spectroscopic data. The 1D (^1H, ^{13}C/DEPT) NMR spectra of **2** (see Section 4) are similar to those of hypothemycin **1**, except for the presence of signals for an additional methyl group at δ 3.36 in ^1H NMR and 58.8 in ^{13}C NMR. The 2D (COSY, HMQC, HMBC) NMR data allowed the unambiguous assignment of all carbon atoms as shown in structure **2**. In particular, the position of the methyl group at 5′-OH was deduced by the correlation of the signal at $\delta = 3.36$ ppm to C-5′. Therefore, the structure of **2** was determined to be 5′-*O*-methylhypothemycin. On the basis of the specific rotation value similar to that of **1** (see Section 4) and on biosynthetic considerations, the absolute configuration may be similarly assigned as (1′*R*,2′*R*,4′*S*,5′*S*,10′*S*)-**2**. The known steroid ergosterol **3** was identified by comparison with published data.[30]

3. Conclusion

In conclusion, the absolute configuration of hypothemycin **1** was assigned by means of our solid-state CD/TDDFT approach, that is, by comparing the CD spectrum recorded in the solid state with that computed with the TDDFT method at the B3LYP/TZVP level. In addition, the family of the resorcylic acid macrolactones was enlarged by new 5′-*O*-methylhypothemycin **2**. The intermolecular interactions of various chromophoric units in the crystals of **1** were recognized as being responsible for the minor discrepancies observed between experimental CD spectra and calculated ones (on a single molecule). Thus far, the presence of such strong chromophoric systems has not hampered the application of our approach for absolute configurational assignments; however, it must always be considered as a potential source of spectral features impossible to predict by single molecule calculations.

4. Experimental

For general methods and instrumentation see the literature[31] and for microbiological methods and conditions of culture see the literature.[32,33] Melting points were determined with a Gallenkamp micro-melting point apparatus and are uncorrected. NMR spectra were run with a Bruker Avance-500 NMR spectrometer with TMS as internal standard. EIMS data were obtained with a MAT 8200 mass spectrometer. The CD spectra were recorded on a J-810 spectropolarimeter. For the solid-state CD protocol, see lit.[17]

4.1. Extraction and isolation

The endophytic fungus *Phoma* sp., internal strain no. 7133, was isolated from *Senecio kleinii* from Gomera and cultivated on 4 L of 5% w/v biomalt solid agar medium at room temperature for 28 days. The culture media were then extracted with ethyl acetate to afford 4.3 g of a residue after removal of the solvent under reduced pressure. The extract was separated into three fractions by column chromatography (CC) on silica gel (170 g), using gradients of *n*-hexane/ethyl acetate (90:10, 50:50, 0:100). The polar fraction (fraction 4) eluted with *n*-hexane–ethyl acetate (2:1) to give crude compound **1** and pure compound **2** (4.5 mg). Crude compound **1** was then recrystallized from *n*-hexane–ethyl acetate to give the pure natural product **1** (30 mg). Fraction 3 was separated by CC on silica gel with *n*-hexane–ethyl acetate (8.5:1.5) to give compound **3** (14 mg).

4.2. Hypothemycin 1

Colorless crystals, mp 174 °C (lit.[2] 173–174 °C, lit.[6] 170–172 °C); $[\alpha]_D^{20} = +18$ (*c* 0.50, $CHCl_3$) {lit.[5] $[\alpha]_D^{24} = +17.4$ (*c* 0.50, $CHCl_3$), lit.[6] $[\alpha]_D^{25} = +18$ (*c* 0.50, $CHCl_3$)}; UV solvent λ_{max}, nm ($\log\varepsilon$): 307, 265, 220; CD (MeCN, $c = 4.14 \times 10^{-4}$) λ ($\Delta\varepsilon$) = 333 (0.92), 305 (−1.89), 261 (−10.94), 234 (9.20), 213 (24.51). CD (KCl) λ (mdeg): 342 (1.44), 323 (−0.86), 299 (1.38), 263 (−8.94), 237 (5.46), 225 (−2.50), 209 (15.16). CD (KBr) λ (mdeg): 338 (1.32), 317 (−1.03), 294 (0.59), 264 (−8.92), 237 (5.32), 227 (−1.84). IR ν_{max} ($CHCl_3$): 3340, 1690, 1650, 1620, 1580; ^{1}H NMR (500 MHz, $CDCl_3$): δ 12.1 (s, 1H, 2-OH), 6.43 (d, $J = 2.0$ Hz, 1H, H-5), 6.41 (d, $J = 2.0$ Hz, 1H, H-3), 6.40 (d, $J = 11.2$ Hz, 1H, H-7′), 6.23 (ddd, $J = 11.2$, 6.6, 4.4, Hz, 1H, H-8′), 5.61 (m, 1H, H-10′), 4.60 (d, $J = 4.5$ Hz, 1H, H-5′), 4.40 (d, $J = 1.7$ Hz, 1H, H-1′), 4.04 (m, 1H, H-4′), 3.80 (s, 3H, 4-OCH_3), 3.01 (ddd, $J = 16.2$, 11.4, 11.4 Hz, 1H, H-9′a), 2.93 (dd, $J = 9.2$, 1.7 Hz, 1H, H-2′), 2.56 (ddd, $J = 16.2$, 2.7, 2.2 Hz, 1H, H-9′b), 1.87 (dd, $J = 15.1$, 9.2 Hz, 1H, H-3′a), 1.48 (d, $J = 6.6$ Hz, 3H, CH_3-10′), 1.13 (dd, $J = 15.1$, 9.2 Hz, 1H, H-3′a); ^{13}C NMR (125 MHz, $CDCl_3$): δ 197.2 (C-6′), 170.8 (*C*OO), 165.6 (C-4), 165.0 (C-2), 143.6 (C-8′), 141.9 (C-6), 129.3 (C-7′), 104.4 (C-1), 104.1 (C-5), 80.9 (C-5′), 71.1 (C-4′), 71.0 (C-10′), 62.5 (C-2′), 59.0 (C-1′), 55.5 (4-OCH_3), 37.8 (C-9′), 34.9 (C-3′), 19.0 (10′-CH_3); HREIMS: *m*/*z* 378.1291 (Calcd. 378.1315 for $C_{19}H_{22}O_8$).

4.3. 5′-*O*-Methylhypothemycin 2

Colorless crystals, mp 161–162 °C; $[\alpha]_D^{20} = +21.0$ (*c* 0.50, $CHCl_3$, 5% CH_3OH); UV λ_{max}, nm ($\log\varepsilon$): 307, 265, 220; IR ν_{max} ($CHCl_3$): 3330, 1685, 1650, 1620, 1580; ^{1}H NMR (500 MHz, $CDCl_3 + CD_3OD$): δ 6.30 (d, $J = 2.1$ Hz, 1H, H-5), 6.28 (d, $J = 2.1$ Hz, 1H, H-3), 6.26 (d, $J = 11.2$ Hz, 1H, H-7′), 6.04 (ddd, $J = 11.2$, 6.5, 4.3 Hz, 1H, H-8′), 5.41 (m, 1H, H-10′), 4.31 (d, $J = 1.7$ Hz, 1H, H-1′), 4.10 (d, $J = 4.5$ Hz, 1H, H-5′), 3.93 (m, 1H, H-4′), 3.80 (s, 3H, 4-OCH_3), 3.96 (ddd, $J = 16.2$, 11.4, 11.4 Hz, 1H, H-9′a), 3.36 (s, 3H, 5′-OCH_3), 2.76 (dd, $J = 9.2$, 1.7 Hz,1H, H-2′), 2.50 (ddd, $J = 16.2$, 2.7, 2.2 Hz, 1H, H-9′b), 1.81 (dd, $J = 15.3$, 9.1 Hz, 1H, H-3′a), 1.32 (d, $J = 6.5$ Hz, 3H, CH_3-10′), 1.03 (dd, $J = 15.3$, 9.1 Hz, 1H, H-3′a); ^{13}C NMR (125 MHz, $CDCl_3 + CD_3OD$): δ 199.9 (C-6′), 171.1 (*C*OO), 165.5 (C-4), 165.0 (C-2), 143.9 (C-8′), 142.2 (C-6), 127.5 (C-7′), 104.1 (C-5), 103.9 (C-1), 90.4 (C-5′), 73.4 (C-10′), 71.1 (C-4′), 62.5 (C-2′), 56.2 (C-1′), 58.8 (5′-OCH_3), 55.4 (4-OCH_3), 36.5 (C-9′), 33.8 (C-3′), 19.0 (10′-CH_3); HREIMS: *m*/*z* 392.1461 (Calcd. 392.1471 for $C_{20}H_{24}O_8$).

4.4. Computational section

MMFF conformational searches were run with the Monte-Carlo algorithm included in the Spartan'06 program (Wavefunction, Inc., Irvine CA, 2006), using default parameters and convergence criteria. AM1 geometry optimizations were run on all conformers obtained through MMFF conformational search within 10 kcal/mol.

DFT and TDDFT calculations were run with the Gaussian'03 program (Gaussian, Inc., Pittsburgh PA, 2003). The input geometry for TDDFT calculations was obtained from the solid-state structure upon re-optimization of the H-atoms' positions with DFT method at B3LYP/6-31G(d) level. TDDFT calculations were executed employing the hybrid functionals B3LYP and PBE0 (PBE1PBE), and Ahlrich's TZVP basis sets.[28]

CD spectra were generated using rotational strengths computed with dipole-length gauge formulation[21,34] to which a Gaussian band-shape was applied with a fixed half-height width between 2500 and 3650 cm^{-1}. Rotational strengths computed with dipole-velocity gauge formulation differed from dipole-length values by less than 15% for most transitions.

Acknowledgements

We thank BASF AG and the BMBF (Bundesministerium für Bildung und Forschung, Project No. 03F0360A), and S. Antus and T. Kurtán thank the Hungarian Scientific Research Fund (OTKA, T-049436, F-043536, NI-61336) for financial support.

References

1. Part 29: Krohn, K.; Zia-Ullah, Hussain, H.; Floerke, U.; Schulz, B.; Draeger, S.; Pescitelli, G.; Salvaderi, P.; Antus, S.; Kurtán, T. *Chirality* **2007**, *19*, 464–470.
2. Nair, M. S. R.; Carey, S. T. *Tetrahedron* **1980**, *21*, 2011–2021.
3. Nair, M. S. R.; Carey, S. T.; James, J. C. *Tetrahedron* **1981**, *37*, 2445–2449.
4. Wee, J. L.; Sundermann, K.; Licari, P.; Galazzo, J. *J. Nat. Prod.* **2006**, *69*, 1456–1459.
5. Agatsuma, T.; Takahashi, A.; Kabuto, C.; Nozoe, S. *Chem. Pharm. Bull.* **1993**, *41*, 373–375.
6. Isaka, M.; Suyarnsestakorn, C.; Tanticharoen, M. *J. Org. Chem.* **2002**, *67*, 1561–1566.
7. Schirmer, A.; Kennedy, J.; Murli, S.; Reid, R.; Santi, D. V. *Proc. Natl. Acad. Sci. U.S.A.* **2006**, *103*, 4234–4239.
8. Tanaka, H.; Nishida, K.; Sugita, N.; Yoshioka, T. *Jpn. J. Cancer Res.* **1999**, *90*, 1139–1145.

9. Zhao, A.; Lee, S. H.; Mojena, M.; Jenkins, R. G.; Patrick, D. R.; Huber, H. E.; Goetz, M. A.; Hensens, O. D.; Zink, D. L.; Vilella, D.; Dombrowski, A. W.; Lingham, R. B. *J. Antibiot.* **1999**, *52*, 1086–1094.
10. Robinson, M. J.; Cobb, M. H. *Curr. Opin. Cell. Biol.* **1997**, *9*, 180–186.
11. Schaeffer, H. J.; Weber, M. J. *Mol. Cell. Biol.* **1999**, *19*, 2435–2444.
12. Kolch, W. *Biochem. J.* **2000**, *351*, 289–305.
13. Cowley, S.; Paterson, H.; Kemp, P.; Marshall, C. *Cell* **1994**, *77*, 841–852.
14. Tatsuta, K.; Takano, S.; Sato, T.; Nakano, S. *Chem. Lett.* **2001**, 172–173.
15. Selles, P.; Lett, R. *Tetrahedron Lett.* **2002**, *43*, 4627–4631.
16. Dai, J.; Krohn, K.; Gehle, D.; Kock, I.; Flörke, U.; Aust, H.-J.; Draeger, S.; Schulz, B.; Rheinheimer, J. *Eur. J. Org. Chem.* **2005**, 4009–4016.
17. Hussain, H.; Krohn, K.; Flörke, U.; Schulz, B.; Draeger, S.; Pescitelli, G.; Antus, S.; Kurtán, T. *Eur. J. Org. Chem.* **2007**, 292–295.
18. Krohn, K.; Kock, I.; Elsässer, B.; Flörke, U.; Schulz, B.; Draeger, S.; Pescitelli, G.; Antus, S.; Kurtán, T. *Eur. J. Org. Chem.* **2007**, 1123–1129.
19. Dreuw, A.; Head-Gordon, M. *Chem. Rev.* **2005**, *105*, 4009–4037.
20. Marques, M. A. L.; Gross, E. K. U. A Primer in Density Functional Theory. In *Time-Dependent Density Functional Theory*; Fiolhais, C., Nogueira, F., Marques, M. A. L., Eds.; Lecture Notes in Physics; Springer: Berlin, 2003; Vol. 620, pp 144–184.
21. Diedrich, C.; Grimme, S. *J. Phys. Chem. A* **2003**, *107*, 2524–2539.
22. Crawford, T. D. *Theor. Chem. Acc.* **2006**, *115*, 227–245.
23. Bringmann, G.; Busemann, S. The Quantum Mechanical Calculation of CD Spectra: The Absolute Configuration of Chiral Compounds from Natural or Synthetic Origin. In *Natural Product Analysis, Chromatography, Spectroscopy, Biological Testing*; Schreier, P., Herderich, M., Humpf, H.-U., Schwab, W., Eds.; Vieweg & Sohn Verlagsgesellschaft: Braunschweig/Wiesbaden, 1998; pp 195–211.
24. Kuroda, R.; Honma, T. *Chirality* **2000**, *12*, 269–277.
25. Kuroda, R. Solid-state CD: Application to Inorganic and Organic Chemistry. In *Circular Dichroism*; Berova, N., Nakanishi, K., Woody, R. W., Eds.; Wiley-VCH: New York, 2000; pp 159–184.
26. Mason, S. F. *Molecular Optical Activity and the Chiral Discrimination*; Cambridge University Press: Cambridge, 1982.
27. Full crystallographic data (excluding structure factors) for **1** have been deposited with the Cambridge Crystallographic Data Centre as supplementary publication no. CCDC-630071. Copies of the data can be obtained free of charge on application to CCDC, 12 Union Road, Cambridge CB2 1EZ, UK (fax: (+44)1223-336-033; e-mail: deposit@ccdc.cam.ac.uk).
28. See Gaussian'03 documentation at http://www.gaussian.com/g_ur/g03mantop.htm for details on basis sets and DFT functionals.
29. Casida, M. E.; Jamorski, C.; Casida, K. C.; Salahub, D. R. *J. Chem. Phys.* **1998**, *108*, 4439–4449.
30. Goulston, G.; Mercer, E. I.; Goad, L. J. *Phytochemistry* **1975**, *14*, 457–462.
31. Dai, J.; Krohn, K.; Gehle, G.; Kock, I.; Flörke, U.; Aust, H.-J.; Draeger, S.; Schulz, B.; Rheinheimer, J. *Eur. J. Org. Chem.* **2005**, 4009–4016.
32. Krohn, K.; Flörke, U.; Rao, M. S.; Steingröver, K.; Aust, H.-J.; Draeger, S.; Schulz, B. *Nat. Prod. Lett.* **2001**, *15*, 353–361.
33. Schulz, B.; Sucker, J.; Aust, H.-J.; Krohn, K.; Ludewig, K.; Jones, P. G.; Doering, D. *Mycol. Res.* **1995**, *99*, 1007–1015.
34. Pecul, M.; Ruud, K.; Helgaker, T. *Chem. Phys. Lett.* **2004**, *388*, 110–119.